Journal of Experimental Marine Biology and Ecology 561 (2023) 151870

Contents lists available at ScienceDirect

Journal of Experimental Marine Biology and Ecology

journal homepage: www.elsevier.com/locate/jembe

Effects of arborescent octocoral assemblages on the understory benthic communities of shallow Caribbean reefs

John F. Girard [*,1], Peter J. Edmunds

California State University Northridge, 18111 Nordhoff Street, Northridge, CA 91330, United States

ARTICLE INFO

Keywords:
Coral reef
Octocoral forest
Ecosystem engineer
Invertebrate community
Sunfleck
Photosynthetic induction

ABSTRACT

Since about 2000, octocorals on the shallow reefs of St. John, US Virgin Islands, have increased in abundance to form dense stands analogous to terrestrial forests. In this study, the ecology of octocoral forests was explored by testing for an effect of their canopies on the light regime and benthic invertebrate community in the understory habitat. Octocoral forests at five sites (7–13 m depth) were quantified on a spatial scale of meters by the height and density of octocoral colonies. Their effects on the understory habitat were evaluated through measurements of downwelling light, benthic invertebrate community structure, and the photophysiology (i.e., induction time) of the common coral, *Porites astreoides* (Lamarck, 1816). Octocoral forests composed of dense (> 5 octocorals m^{-2}) and tall (mean height of 42 cm) octocoral colonies created an understory habitat characterized by flashes of bright light (i.e., sunflecking). Within the understory habitat at two of three study sites, the community structure of benthic invertebrates was modified by the octocoral canopy, but it remained unaffected at a third site. A test for the effects of sunflecking on the induction time of *P. astreoides* found no difference between colonies in the understory versus the open reef habitat. These results do not support the notion that the physiological phenotype of autotrophs in the understory habitat is modified to exploit sunflecking. The analysis of the benthic invertebrates in the understory habitat suggests that octocoral forests can change the community structure of this group of organisms, relative to the open reef. The causes of this change are unclear, but its absence at the most sheltered study site suggests that water motion may be a contributing factor. The strong likelihood that octocoral forests mediate ecologically significant changes in the community structure of invertebrates within their understory habitat warrants further investigation.

1. Introduction

In ecology, ecosystem engineers profoundly change the structure and function of ecosystems through modification of the physical (autogenic), or chemical (allogenic) features of habitats (Jones et al., 1994; Kern et al., 2013). The outcome of these effects modify species interactions (Guy-Haim et al., 2018; Siebert and Branch, 2006), and can create distinctive communities (Jones et al., 1994; Fox and Bellwood, 2013; Guy-Haim et al., 2018) as occurs with mature trees in terrestrial forests (Hilmers et al., 2018), and the shaded understory habitat they create (Chazdon and Pearcy, 1991; Hilmers et al., 2018; Brunel et al., 2020). The "forest" construct has been extended to the marine environment, where functional analogues of forests are created by a variety of organisms including seagrasses, corals, and kelp (Jones et al., 1994; Siebert and Branch, 2006; Rossi et al., 2017; Miller et al., 2018; Shelamoff et al., 2019) .

Marine animal forests operate in a viscous fluid with physico-chemical features affecting the morphology of sessile organisms from which forests arise (Denny et al., 1985; Atkinson and Falter, 2003; Monismith, 2007). Interactions between organisms and their flow environments affect food availability (Abelson et al., 1993), particle capture (Okamura, 1984, 1985; Helmuth and Sebens, 1993; Sebens et al., 1997), the likelihood of breakage or dislodgement from the substratum (Koehl, 1982; Madin et al., 2014), and the capacity to exchange metabolites with seawater (Ackerman and Okubot, 1993; Nishizaki and Carrington, 2014). Modifications of seawater flow are likely to be a primary mechanism through which octocorals forests influence organisms living beneath their canopies in the understory habitat. Examples of the aforementioned effects have started to emerge for octocoral forests (see Lasker et al., 2020b; Cerpovicz and Lasker, 2021), and they

* Corresponding author.
E-mail address: John_Girard@uri.edu (J.F. Girard).
[1] Current address: University of Rhode Island, 45 Upper College Road, Kingston, RI 02881, United States.

https://doi.org/10.1016/j.jembe.2023.151870
Received 19 April 2021; Received in revised form 2 January 2023; Accepted 9 January 2023
Available online 20 January 2023

augment a rich literature on this topic for other organisms (Lin and Dai, 1996; Ghisalberti and Nepf, 2006; Luhar and Nepf, 2011; Nepf, 2012a; Lowe and Falter, 2015).

In addition to flow, canopies formed by benthic organisms in aquatic habitats also affect the quantity (i.e., photon flux density, PFD) and quality (spectral composition) of light reaching the understory habitat (Gerard, 1984; Tomasko, 1992), which can affect photosynthetic rates of understory organisms (Collier et al., 2012) and settlemt choice (Thorson, 1964). Light can be quantitatively modified through shading (Stewart et al., 2007; Giuliani and Brown, 2008), wave focusing (Stramska and Dickey, 1998), and sunflecking caused by canopy motion (Gerard, 1984; Wing et al., 1993). Qualitatively, light can be altered by the absorptivity of water (Kirk, 1977) and pigments associated with the canopy through which light is filtered (Nobel, 2020). In response to these effects, members of the photosynthetic understory community typically optimize rates of photosynthesis at low light quantity (Nobel, 2020), avoid photodamage at high light quantity (Nobel, 2020), and efficiently utilize sunflecks (Kaiser et al., 2015). Photosynthetic organisms in an understory typically exhibit shade adaptation (Todd, 2008; Nobel, 2020), and similar trends are likely to be found in organisms in the understory habitat beneath octocorals forests.

The biological effects of sunflecking are under studied in marine environments (Gerard, 1984; Wing et al., 1993; Wing and Patterson, 1993), although they are well known for terrestrial forests (e.g., Chazdon and Fetcher, 1984; Pearcy, 1988; Chazdon and Pearcy, 1991). This is unfortunate, as highly dynamic light environments characterize many shallow marine environments (Wing and Patterson, 1993) and it is likely that photosynthetic organisms can respond in beneficial ways to these effects (Kaiser et al., 2017; Nobel, 2020). In response to rapidly (seconds) fluctuating light quantity, algal photophysiology can reduce the time required to achieve maximum photosynthesis (i.e., induction time, (Osterhout and Haas, 1918; Clendenning and Haxo, 1956)) at a given PFD (Pahl-wostl and Imboden, 1990). Because up to 80% of daily light quantity can be delivered to the understory habitat by sunflecks, at least in terrestrial forests (Chazdon and Fetcher, 1984), the capacity to photosynthetically exploit this source of energy is likely to have ecological importance in marine animal forests.

The concept of animal forests (Rossi et al., 2017) are well matched to dense stands of arborescent octocorals on Caribbean reefs (Lasker et al., 2020b). Octocorals have long been common on shallow reefs in the Caribbean (Cary, 1914; Kinzie, 1973), yet recently have increased in abundance (Ruzicka et al., 2013; Lenz et al., 2015; Edmunds and Lasker, 2016). This trend appears to be part of a suite of events affecting reefs in this region, which include a shift in functional dominance from scleractinians to macroalgae (Kramer et al., 2003; Mumby, 2009) that constitutes a change in ecological phase, or possibly an alternative stable state (sensu Fung et al., 2011). The shallow reefs of St. John, US Virgin Islands, have been a focus for describing these changes for decades (Tsounis and Edmunds, 2017), and by 2015 it was clear that at least some of the reefs had transitioned to high abundance of octocorals (Lenz et al., 2015; Edmunds et al., 2016; Tsounis and Edmunds, 2017). The octocoral communities appear to be more resilient to environmental challenges than the scleractinian communities they replace (Tsounis and Edmunds, 2017; Lasker et al., 2020a), and may represent a new "normal" for shallow (i.e., < 15 m depth) Caribbean reefs (Lasker et al., 2020a).

This study investigated the ecological consequences of the formation of animal forests by arborescent octocorals on the shallow reefs of St. John. Initially, the light beneath octocoral canopies was quantified to determine whether illuminance delivery differed from the open reef through sunflecking. Then we tested two hypotheses: (1) there is no association between the physical attributes of octocoral canopies and the community of benthic invertebrates living in the understory habitat, and (2) photosynthetic induction of the coral, *Porites astreoides* (Lamarck, 1816), is unaffected by sunflecking beneath octocoral canopies. To test these hypotheses, we explored the relationship between forest metrics (i.e., density and height of octocoral colonies), and the closure of their canopies (sensu Jennings et al., 1999), and the invertebrate community within the understory habitat. We did not measure seawater flow and light attenuation as potential mechanisms mediating changes in the invertebrate communities as these effects have been demonstrated in the aforementioned work. We chose instead, to focus on an under studied mechanism (i.e., sunflecking) by which canopies could mediate effects on one type of understory organism (i.e., those exploiting autotrophic nutrition).

2. Methods

2.1. Overview

Research was conducted on the shallow reefs (≤ 13-m depth) along the south shore of St. John in 2019 (March, July, and August), and 2020 (January). Surveys were completed at five sites between White Point and East Cabritte that sampled a natural gradient in the extent to which octocorals form canopies. Although testing of our key hypotheses would have benefitted from a contrast of a fully open reef community (i.e., without arborescent octocorals) and a densely forested reef, preliminary surveys indicated that arborescent octocorals were present in at least low densities on all our study reefs (i.e., arborescent colonies were present on all reef surfaces, albeit sometimes at low densities). Therefore, the study tested the effects of octocorals along a gradient of octocoral densities extending from low (~ 1 octocorals m^{-2}) to high (17 octocorals m^{-2}) density. The five sites were separated from each other by ~500 m, and were distributed along ~1.5 km of coast between Cabritte Horn and White Point (Fig. 1). Each site was sampled using quadrats (1 × 1 m), which served as the statistical replicates for all analyses.

The octocoral canopy was characterized by the mean height and density of octocorals with holdfasts in each quadrat, as well as the extent to which the canopy occluded downwelling light (hereafter, canopy closure [sensu Jennings et al., 1999]). The dependent variables used to test each hypothesis were measured separately in subsets of quadrats because it was not possible to simultaneously sample the reef to test multiple hypotheses. To quantify the effects of the octocoral canopy on the light regime and benthic community composition, quadrats were randomly placed along 20 m, non-overlapping transects that were

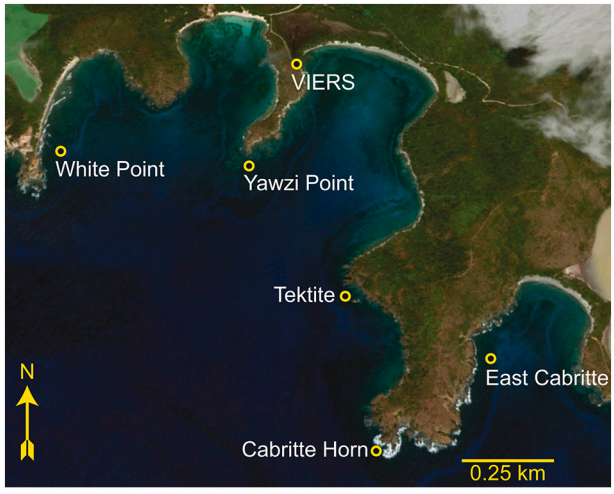

Fig. 1. Map of study sites along the south shore of St. John, US Virgin Islands, between Europa Bay (left) and Grootpan Bay (right). Sites indicated by circles, "VIERS" shows the location of the Virgin Islands Ecological Research Station. Map image Google Earth Pro 7.3.4.8573 , *Lameshur Bay St. John US Virgin Islands 18°18'43.38"N, 64°43'26.93"W, elevation 1.70km*. photo date 13/Aug/2009.

positioned haphazardly along fringing reefs at a depth of 9 ± 2 m (mean ± SD, range 7–13 m). Quadrats were placed along the transects at random positions constrained to roughly horizontal surfaces on hard substrata within the chosen depth range. As some sites were easier to access than others, sample sizes (number of quadrats) were unbalanced among sites.

Sampling included octocorals >5 cm tall with holdfasts within each quadrat. The height (± 0.5 cm with a 50 cm ruler) and density (octocorals m^{-2}) of all such octocorals was measured. Analyses were constrained to octocorals >5 cm tall because these are likely to be adults (Lasker et al., 2020a), and because short octocorals cannot contribute to canopy structure when this feature is constructed by adjacent taller octocorals. The encrusting octocoral *Erythropodium caribaeorum* (Duchassaing and Michelotti, 1860) was included in surveys focused on community structure, but excluded from surveys focused on canopy features because it does not form arborescent colonies. Canopy closure was expressed as a percentage of the sky that was obscured by the canopy when viewed from the benthos.

In terrestrial forests, canopy closure is measured using hemispheric photography (Jennings et al., 1999) in which a camera with a 180° field of view is placed on the substratum beneath the canopy with the lens oriented perpendicular to the sky. The digital image from this position is analyzed to determine the proportion of pixels classified as "clear" relative to the white, downwelling light. In the present study, canopy closure beneath octocoral forests was measuring using a GoPro Hero 3+ camera with a 130° field of view (manufacturer's specification, GoPro, 2013, Inc. San Mateo, CA). This camera was used to record still images in the center, and at each of the four corners, of quadrats, with all five images $quadrat^{-1}$ recorded within <5 min. To avoid biases in estimating canopy closure caused by adjacent non-living substrata (e.g., boulders and rock walls), images were excluded when they included these features. Images were analyzed using ImageJ software (v1.52a, Schneider et al., 2012), in which 300 randomly located dots (~ 0.5 pixel in diameter) were superimposed on each image. The number of dots on the octocoral canopy were counted and expressed as a percentage of the dot population. This metric was used to quantify canopy closure, and the results from the five images $quadrat^{-1}$ were averaged to characterize each quadrat.

2.2. Light regime beneath canopies

Downwelling light was measured beneath the canopies using HOBO light loggers (model UA-002-64) recording in lux (sensitive to 150–1200 nm wavelength of light), and sampling at 1 Hz from ~05:00 to ~18:00 h. Loggers were deployed for a single day in either East Cabritte (9 m depth) or Yawzi Point (8 m depth) during March 2019, and each deployment involved a paired contrast of a sparse octocoral canopy (n = 2 loggers) versus a dense octocoral canopy (n = 3 loggers). All deployments occurred on representative summer days characterized by sunshine and scattered clouds, and low wind speeds of ~6.0–8.5 m s^{-1} (CariCOOS buoy 41052, ~ 8 km SW of Cabritte Horn). Given the availability of a fixed number of loggers, their placement within dense canopies was prioritized over areas of sparse canopy to accurately quantify the canopy effect on the light regime beneath. Each logger was secured in the center of a quadrat, in which octocorals were censused (described above), and a level was used to fix the sensor perpendicular to the horizon. Each logger was treated as an independent replicate (the design was unbalanced with respect to sampling in the dense canopies) and data were processed using spectral analysis (section 2.5.1).

To assist in the ecological interpretation of variation in illuminance (Lux) relative to photosynthetically active radiation (PAR, 400–700 nm), a HOBO light logger was cross calibrated (after Long et al., 2012) against a cosine-corrected PAR sensor (LI-192, Li-Cor Biosciences) fitted by the manufacturer into a logger (miniPAR, Precision Measurement Engineering). In January 2021, the two loggers were simultaneously deployed at 9 m depth in St. John, where they synchronously sampled at 0.0017 Hz. The relationship between Lux and PAR was determined by least squares regression.

2.3. Community beneath canopy

In the quadrats sampled to test for an association between the octocoral canopy and the benthic community, macroscopic benthic invertebrates (i.e., > ~ 0.5 cm in length) were surveyed in situ without removing organisms or overturning substrata. Mobile and sessile taxa were counted, and analyses resolved organisms to the lowest taxonomic level possible without collecting voucher specimens. Arborescent octocorals were excluded as they represented the contrast of a the canopy effect. Unitary organisms were recorded as individuals, and encrusting modular organisms were counted by the number of autonomous patches of biomass, with both expressed as organisms $quadrat^{-1}$. Organisms were identified in situ or with reference photos (18.2 megapixels) using field guides (Humann et al., 2013), expert opinion (mostly for sponges), and an electronic reference catalog (Zea et al., 2014). Surveys were conducted at Cabritte Horn, Tektite, and White Point (Fig. 1).

2.4. Induction time

To test the hypothesis that the induction time in *Porites astreoides* was affected by octocoral canopies, corals were haphazardly selected in the understory habitat of high density octocoral forests, and areas of reef where octocorals were sparse. Induction time was quantified using chlorophyll fluorescence (Genty et al., 1989). To avoid the confounding influence of depth-dependent reductions of PFD on induction time (Macintyre et al., 2000), measurements were made on corals located within a depth range (~ 7.0 ± 0.5 m) that was narrower than that used to quantify the canopy effect on benthic invertebrates. Colonies were categorized as within dense canopies if they were shaded by at least one octocoral colony ≥25 cm tall when it flexed in routine oscillatory water flow. Preliminary surveys showed that colonies of *P. astreoides* met this criterion when the distance from the nearest tall octocoral was less than half the height of the octocoral colony. The distance between *P. astreoides* colonies and the nearest octocoral was measured to categorize colonies of *P. astreoides* as within or outside the understory habitat. A single induction curve was performed on each *P. astreoides* on one of 16 days during July and August 2019. Sampled colonies were >4 cm in diameter to provide space on the colony surface for the placement of the fiber-optic probe (5 mm diameter) attached to the Diving Pulse Amplitude-Modulation (PAM) fluorometer (Heinz Walz, GmbH) that was used to measure induction time.

To quantify induction time, the time to steady state photosynthesis was measured by evaluating the performance of photosystem II (PSII) using chlorophyll fluorescence (Bradbury and Baker, 1984, 1981). Calculation of the rate of production of high energy electrons by PSII (relative electron transfer rate, rETR) at a fixed PFD is a measure of induction time (Suggett et al., 2010). rETR was calculated using the manufacturers software (Eq. 1):

$$rETR = \frac{\Delta F}{Fm} \times PAR \times 0.5 \times 0.001 \quad (1)$$

where ΔF is the change in fluorescence (F) resulting from the saturation pulse, F_m is the maximum fluorescence, PAR is the PFD to which the sample is exposed, 0.5 is an estimate of the quanta absorbed by PSII, and 0.001 is an absorptance constant for light at the coral surface. As neither the absorptance of light by the coral surface, nor quanta by PSII, are known *for P. astreoides*, this equation estimates relative ETR.

Typically, induction is quantified using an induction curve (sensu Genty et al., 1989), in which rETR is expressed as a function of time under exposure to a fixed PFD (Zipperlen and Press, 1997). The PFD employed is usually an ecologically relevant value experienced by the organism in situ, or the saturating irradiance (Pearcy et al., 1985;

Zipperlen and Press, 1997). In the present study, the actinic light administered by the PAM was adjusted to ~896 μmol photons m^{-2} s^{-1} to mimic the maximum PFD at the study depth, as determined by local records of the diffuse attenuation coefficient (K_d) (Edmunds et al., 2018) and surface PFD for July – August 2018. Calculations from these data show maximum PFD ranged from ~737–1178 μmol photons m^{-2} s^{-1} at 7 m depth in Great Lameshur Bay. In the laboratory, induction curves usually are prepared using dark-adapted organisms (Genty et al., 1989), but in situ they typically are prepared for organisms having a common light history obtained by sampling at a fixed time of day (Poorter and Oberbauer, 1993). Therefore, all colonies were measured between 09:00 and 11:00 h, on clear cloudless days, to standardize the ambient light regime to which they were exposed prior to analyses. Induction curves were prepared using the manufacturers protocol for the Diving PAM (Heinz Walz, 1998), in which actinic light is consistently delivered for 17 min, and rETR is measured through the delivery of 13 saturating pulses every 1.4 min.

2.5. Statistical analysis

2.5.1. Light regime beneath canopies

Spectral analysis of illuminance was used to determine the dominant spectral peaks associated with downwelling light. Time series of illuminance extended from dawn to dusk, or until the loggers were collected on the same day (ca 15:30 h), whichever was shorter. Time series were filtered to remove means and linear trends, and each series was zero padded to the nearest power of two (Emery and Thomson, 2014) prior to spectral analysis using a Fast Fourier Transformation (FFT). Periodograms were used to identify dominant spectral peaks and were smoothed by averaging the scores within a window of 35 spectral estimates (i.e., band averaging [Emery and Thomson, 2014]). Dominant peaks were identified based on elevated power spectral density at a given frequency compared to other frequencies around it, where the lowest resolvable frequency (fundamental frequency, f_0) in cycles per second (Hz) was defined as 3/(2 T), where T is the sampling duration in seconds (Emery and Thomson, 2014). The highest resolvable frequency (Hz) was conservatively taken to be $1/(4\Delta t)$, half the Nyquist frequency ($f_N = 1/(2\Delta t)$), where Δt is the sampling interval (Emery and Thomson, 2014). Illuminance delivery was resolved between 5.0×10^{-5}–0.25 Hz at East Cabritte ($T = 33{,}324$ s, $\Delta t = 1$ s), and 3.0×10^{-5}–0.25 Hz at Yawzi Point ($T = 44{,}206$ s, $\Delta t = 1$ s). Periodograms of illuminance beneath and outside of canopies were qualitatively compared to one another at Yawzi Point and East Cabritte. Analyses were completed in the R software environment (v3.6.1; R Foundation for Statistical Computing; http://www.R-project.org/) using the 'spectral' package v 1.3 (Seilmayer, 2019).

2.5.2. Community beneath canopies

Variation in benthic community structure and the octocoral canopy was separately explored with 2-dimensional ordinations completed using non-metric multidimensional scaling (MDS). First, benthic community data were fourth-root transformed to reduce the effects of overrepresented taxa before preparing resemblance matrices for each site using Bray-Curtis dissimilarities (Clarke et al., 2008; Somerfield and Clarke, 2013). Community analyses were completed using all invertebrates encountered in surveys, and they included *E. caribaeorum* but excluded all other octocorals (Table S1). Ordinations were prepared from multiple restarts until stress stabilized. In the ordination plots, significant clusters of quadrats (at $P \leq 0.05$) were identified using similarity profile analysis (SIMPROF, Clarke et al., 2008; Somerfield and Clarke, 2013) with 999 permutations. Where significant clusters were detected, they were displayed with similarity contours.

Second, the variables defining octocoral canopies (e.g., mean closure, density, mean height) were *Z*-score transformed within each site before preparing resemblance matrices using Euclidean distances (Clarke et al., 2008; Somerfield and Clarke, 2013). Thereafter, the ordination was prepared as described above for the benthic community. The test for association between benthic community structure and canopy formation was conducted using BIO-ENV multivariate correlation, with significance evaluated in a permutational framework using 99,999 permutations (after Clarke and Ainsworth, 1993).

Ordinations, multivariate associations, and significance tests were conducted in the R software environment (v3.6.1; R Foundation for Statistical Computing; http://www.R-project.org/) using the packages 'vegan' v2.5–6 (Oksanen et al., 2019), 'clustsig' v1.1 (Whitaker and Christman, 2014), and 'fastcluster' v1.1.25 (Müllner, 2013).

2.5.3. Induction time

rETR for each coral was plotted against exposure time to each PFD, and qualitatively screened for conformity to typical induction responses in marine photosynthetic symbionts (Schreiber et al., 1997). Screening did not reveal any replicates for exclusion from the analysis. The time to steady state photosynthesis (T_i, the induction time) was taken as the intersection on the abscissa of two straight lines, one calculated using least squares linear regression of the first three points on the rETR curve, and the second representing the mean rETR of the last three points of the curve. The first three points represented the most rapid increase in rETR as a function of exposure time, and the last three points operationally defined the maximum rETR, particularly in cases where an asymptotic value was not reached. Using T_i as a dependent variable, a two-way, mixed effects ANOVA was used to test for variation in induction time as a function of canopy (fixed effect) and site (random effect). The assumptions of normality and equal variance were tested through graphical analysis of residuals. Analyses were performed in the R software environment (v3.6.1; R Foundation for Statistical Computing; http://www.R-project.org/), using the packages 'car' v3.0–5 (Fox and Weisberg, 2019) for assumptions tests, and calculation of Type III sums of squares for ANOVAs, and 'stats' (v3.6.1; R Foundation for Statistical Computing; http://www.R-project.org/) for linear model construction and calculation of *P*-values from F-statistics.

3. Results

3.1. Overview

Overall, 714 octocorals from eight genera were measured to test for a relationship between octocoral canopies and benthic invertebrates. The most common octocorals were *Eunicea* (43.4% of colonies), *Gorgonia* (16.1%), *Pseudoplexaura* (15.0%), and *Antillogorgia* (14.8%); *Briareum, Muricea, Plexaurella,* and *Pterogorgia* each represented <4% of the colonies. At Cabritte Horn, Tektite, and White Point, seven genera were found: *Plexaurella* was not recorded at Cabritte Horn, *Pterogorgia* was not recorded at Tektite, and *Briareum* was not recorded at White Point. Together, arborescent octocorals created dense forests (up to 17 octocorals m^{-2}) with canopies extending to 67 cm above the benthos (Fig. 2, Table 1). Mean canopy closure was significantly ($P < 0.05$) associated with octocoral density ($R^2 = 0.30$) and mean canopy height ($R^2 = 0.14$) and both associations were positive (Fig. 3).

The benthic communities were dense and taxonomically rich with 3432 organisms assigned to 118 putative taxa representing 7 phyla, 10 classes, and 82 species. Of the organisms not resolved to species, 27 were sponges (Porifera), 2 were identified to class, 6 to family, and 2 to genus (Tables S1, S2). Within a quadrat, a mean of 19.5 ± 0.6 taxa (± SEM, $n = 67$) was found, and most were poriferans (41.0%) or scleractinians (38.5%). Most sponges were *Monanchora arbuscula* (Duchassaing and Michelotti, 1864) (13.0% of sponges) or *Niphates digitalis* (Lamarck, 1814) (10.2%), and 26% were assigned to one of 27 phenotypically distinct, yet taxonomically undefined groups (Table S1, S2). Based on their phenotypic alignment with recognized species, they were conservatively scored as species but assigned "Unknown identity". Most scleractinians were *Siderastrea siderea* (Ellis and Solander, 1786) (26.5% of scleractinians) and *Porites astreoides* (24.5%). Of the remaining

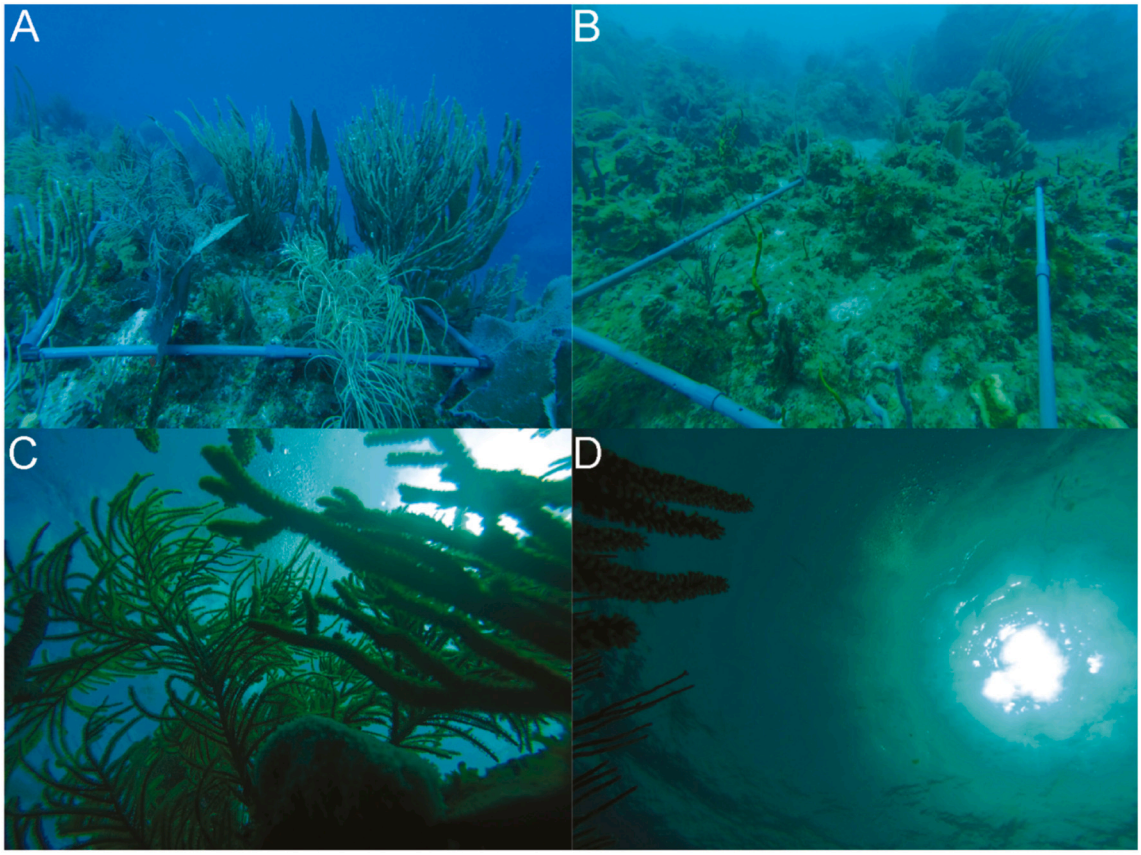

Fig. 2. Photographs of quadrats sampled in Great Lameshur Bay, St. John. Pictures show variation in octocoral forests that were categorized by the combination of canopy structure (mean height, and density) as tall and dense (A), or short and sparse (i.e., outside of dense canopies) (B), and by canopy closure as strong (C) or weak (D).

Table 1
Octocoral canopy metrics from surveys of benthic invertebrate communities and canopy analysis at three sites (Fig. 1) (mean ± SEM, n = number of quadrats).

Site	Height (cm)	Density (individuals m^{-2})	Closure (%)	(n)
Cabritte Horn	27.5 ± 5.3	6.6 ± 0.8	13.4 ± 1.7	25
Tektite	20.0 ± 2.7	4.1 ± 0.6	7.9 ± 1.4	28
White Point	28.0 ± 2.2	6.6 ± 0.5	17.0 ± 2.6	14

invertebrates, 8.5% were cnidarians (other than scleractinians), 5.4% polychaetes, and 6.6% were represented by Echinodermata, Gastropoda, Decapoda, and Ascidiacea together; most invertebrates (95.7%) were sessile.

3.2. Light regime beneath canopies

For the octocoral canopies under which light was measured, canopies categorized as dense at East Cabritte had a mean height of 39.0 ± 5.7 cm, a mean density of 12.3 ± 0.9 individuals m^{-2} (all ± SEM, $n = 3$), and a canopy closure of 31.4 ± 6.1% (± SEM, n = 3). Canopies categorized as sparse had a mean height of 25.7 ± 6.9 cm, a mean density of 4 ± 1 individuals m^{-2} (all ± SEM, $n = 2$), and a canopy closure of 1.2 ± 0.2% (± SEM, n = 2). At Yawzi Point, the equivalent features of dense canopy values were 51.5 ± 2.8 cm, 4.7 ± 0.6 individuals m^{-2} (all ± SEM, n = 3), and 13.1 ± 4.0%, respectively (± SEM, n = 3). Sparse canopies had a mean height of 3.5 ± 3.5 cm, mean density of 0.5 ± 0.5 individuals m^{-2} (all ± SEM, n = 2), and a canopy closure of 1.3 ± 1.3% (± SEM, n = 2).

At East Cabritte, maximum illuminance within sparse octocoral canopies ranged from 31.7 to 37.2 klx, and beneath dense octocoral canopies, from 24.8 to 35.8 klx. At Yawzi Point, maximum illuminance ranged from 40.0 to 46.8 klx within sparse octocoral canopies, to 37.2–44.1 klx beneath dense octocoral canopies. Integrated daily illuminance beneath dense canopies relative to outside of dense octocoral was 36% lower at East Cabritte, and 13% lower at Yawzi Point. Within and outside dense canopies, illuminance greatly varied between measures separated in time by 1 s, but this effect was accentuated beneath dense canopies (Fig. 4).

At East Cabritte, periodograms of illuminance revealed prominent temporal structuring at 0.004 Hz and 0.013 Hz, but beneath dense canopies there was an additional frequency band between 0.100 Hz and 0.160 Hz. Within this band the power spectrum was elevated by an order of magnitude relative to the same frequency band outside dense canopies. At Yawzi Point, the illuminance periodograms beneath the densest canopy had an elevated power spectral band from 0.033 Hz – 0.200 Hz relative to outside dense canopies. This band was not present in the two other illumination periodograms from beneath dense canopies. At East Cabritte and Yawzi Point, high frequency variation in illuminance beneath canopies (versus outside dense canopies) was only evident when octocoral densities were > 5 octocorals m^{-2}.

Based on paired deployments of the HOBO and miniPAR loggers, records on the two measurement scales were related ($r^2 = 0.96$, from $n = 1544$ paired non-zero observations) with a power function:

$$PAR = 0.1175x^{0.9096}$$

where x is illuminance in Lux (by the HOBO logger) and PAR was recorded with the miniPAR logger. The calibration obtained in January 2021 was prepared across an illuminance range of 0–18.6 klx, which is truncated relative to the values recorded in July 2019 (up to 46.8 klx). Based on this relationship, at East Cabritte, maximum illuminance

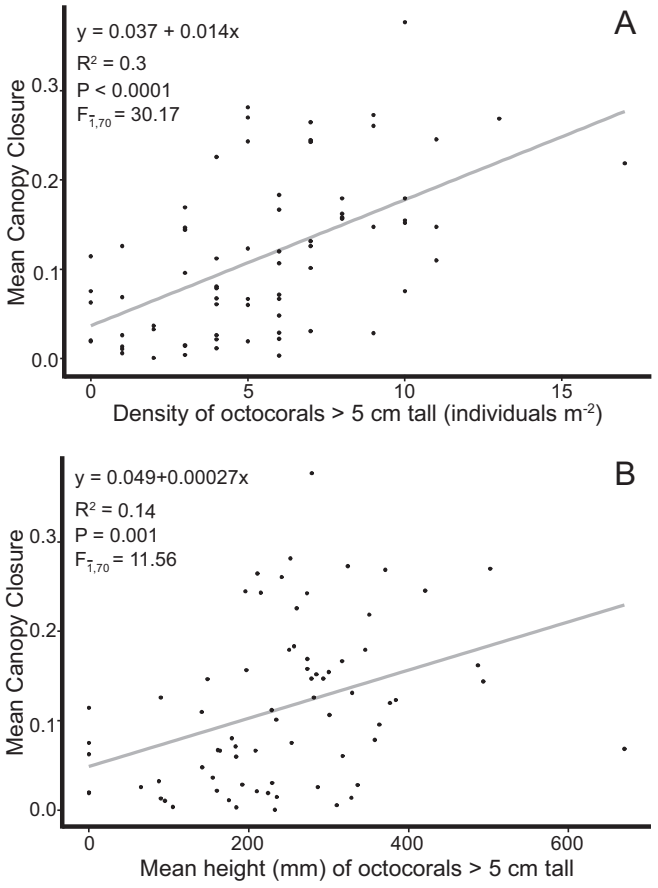

Fig. 3. Scatter plots of (A) octocoral density and (B) mean octocoral height against mean canopy closure within 1 m^2 quadrats. Octocorals <5 cm tall were excluded from analyses. Grey lines represent linear regressions with their statistical support included in the box frame. Octocoral canopy data were pooled across sites where canopy and community metrics were quantified (n = 72 quadrats).

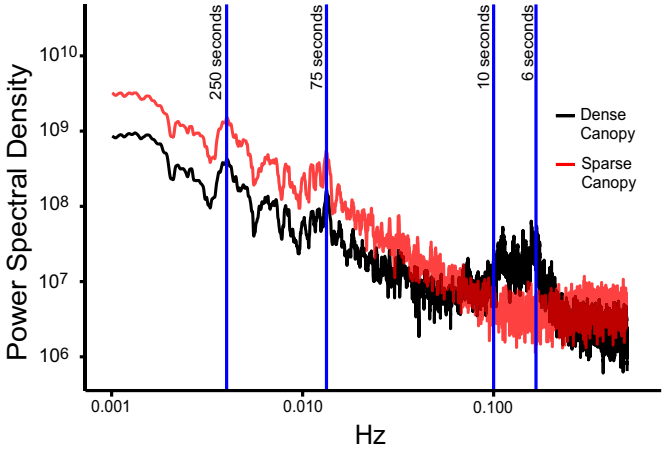

Fig. 4. Representative plot of smoothed spectral density periodograms of the frequencies structuring the illuminance within and outside of dense octocoral canopies at 8–9-m depth. Periodograms were smoothed by band averaging 35 adjacent spectral estimates (Dense canopy $n = 6$, Sparse canopy $n = 4$). Vertical lines are placed on spectral peaks or on the ends of spectral bands (e.g., 6 s – 10 s) that demonstrate elevated power spectral densities compared to surrounding frequencies. Labels next to vertical lines represent their position on the frequency axis expressed as seconds $cycle^{-1}$.

outside octocoral canopies ranged from 1459 to 1688 μmol photons m^{-2} s^{-1} and beneath the octocoral canopy, from 1167 to 1631 μmol photons m^{-2} s^{-1}. At Yawzi Point, maximum illuminance ranged from 1802 to 2082 μmol photons m^{-2} s^{-1} on the open reef, from 1688 to 1970 μmol photons m^{-2} s^{-1} beneath octocoral canopies.

3.3. Community beneath canopies

The physical structure of the octocoral canopies, and the community structure of the understory benthic invertebrates, varied among sites. The canopies formed by octocorals ranged in density from <1 individual m^{-2} to 17 individuals m^{-2}. Overall, mean canopy densities and heights were similar at Cabritte Horn and White Point, but mean canopy height was ~8 cm shorter at Tektite relative to the other two sites (Table 1). At Cabritte Horn, Tektite, and White Point, octocoral canopies were primarily composed of *Eunicea* spp., which made up 44%, 35%, and 45% of octocoral colonies at each site, respectively (n = 106–184 octocorals). The next most abundant taxon at each site was *Pseudoplexaura* spp. at Cabritte Horn (23.9%), *Gorgonia* spp. (31.5%) at Tektite, and *Antillogorgia* spp. (18.9%) at White Point.

For each site, MDS ordinations produced using canopy metrics or benthic community structure qualitatively separated quadrats in clusters throughout ordination space (Fig. 5). Canopy ordinations stabilized in <40 restarts with stress from 0.085 to 0.117. Community ordinations stabilized in <500 restarts with stress from 0.190 to 0.229. For the ordination based on canopy metrics, SIMPROF resolved 2 clusters of quadrats at Cabritte Horn (P_{perm} = 0.019) and 7 at Tektite ($P_{perm} \leq$ 0.031), but no clusters were resolved at White Point (P_{perm} = 0.625) (Fig. 5). For the ordination based on benthic community structure, SIMPROF resolved three clusters of quadrats at Cabritte Horn ($P_{perm} <$ 0.020), and 3 at Tektite ($P_{perm} \leq$ 0.031), but clusters were not resolved at White Point (P_{perm} = 0.503) (Fig. 5). The BIO-ENV tests for association between the resemblance matrices for canopy and community features were significant at Cabritte Horn (P_{perm} = 0.040) and White Point (P_{perm} = 0.049), but not at Tektite (P_{perm} = 0.056) (Table 2). The correlation between canopy features and benthic communities at Cabritte Horn and White Point show that as octocoral forests vary in height, density, and closure, the invertebrate community also changes. At Tektite, variation in these features statistically was independent.

The best-developed examples of the association between octocoral canopy features and benthic communities were provided by *Agaricia agaricites* (Linnaeus, 1758), *Porites astreoides, Siderastrea siderea* (all Scleractinia), *Siphonodictyon coralliphagum* (Rützler, 1971) (Porifera), and *Clavalina picata* (Verrill, 1900) (Tunicata). These taxa were 20–391% more abundant (i.e., increases of ~1–2 individuals m^{-2}) in the understory of dense octocoral canopies versus areas of sparse octocoral canopies. *Monanchora arbuscula* (Porifera) was 21.5% less abundant (i.e., representing ~1 individual m^{-2}) in the understory of dense octocoral canopies versus sparse octocoral canopies. Ultimately, the effect of the octocoral forest on the community structure of invertebrates in the understory habitat was represented by many small, yet consistent changes in the abundances of multiple taxa. For example, the sponge *Cinachyrella kuekenthali* (Uliczka, 1929) was 531% more abundant in the understory habitat beneath dense octocoral canopies compared to areas of sparse octocorals, and this effect was attributed to just one extra sponge in 4 m^2 of substratum beneath dense octocoral canopies. Overall, beneath dense octocoral forests and relative to areas of sparse octocorals, 37 taxa showed small absolute changes in abundance that corresponded to large relative changes in abundance. These effects amounted to increases of ≥100% beneath dense versus sparse canopies, and reductions of ≤50% beneath sparse versus dense canopies (Table S2). At higher taxonomic levels (Table S2), the benthic community beneath dense canopies versus sparse canopies was characterized by ~2.5 more scleractinians, ~1 more poriferans, ~1 more polychaetes, ~1 more ascidians, and ~ 0.5 more molluscs and echinoderms (units: individuals m^{-2}). The benthic community beneath sparse canopies versus dense canopies was

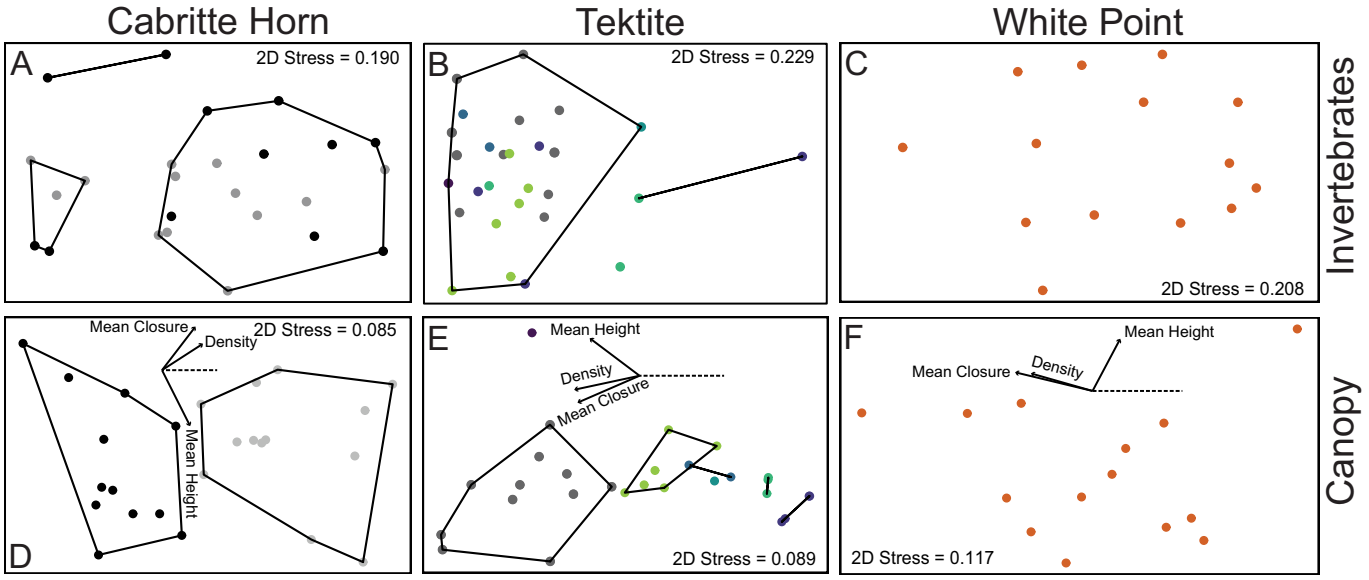

Fig. 5. MDS of benthic invertebrate community abundances (top row A–C, 118 different taxa) and canopy metrics (bottom row D-F, three metrics) from 7 to 1 m depth, at three sites in Great Lameshur Bay (Cabritte Horn $n = 25$, Tektite $n = 28$, White Point $n = 14$). Perimeter hulls surrounding points represent significant clusters as defined by Similarity Profile Analysis (SIMPROF). Point color represents the canopy cluster to which a point belongs. Symbol colors are consistent between MDS plots for community and canopy effects by site. Vectors represent relative correlational strength of canopy metrics (Mean height, Density, Mean closure) with MDS space. Dashed line shows a vector corresponding to $r = 1$ for scale.

Table 2
Results from multivariate correlation tests between resemblance matrices prepared for community structure (by Bray-Curtis dissimilarities) and octocoral canopy metrics (by Euclidean distances) using BIO-ENV spearman rank correlations (r_s, p = probability of association). The resemblance matrices for invertebrates and canopies were based on quadrats as replicates that were sampled at three sites (Fig. 1).

Site	r_s	P
Cabritte Horn	0.149	0.040
Tektite	−0.021	0.564
White Point	0.232	0.049

characterized by ~1 more cnidarians (other than scleractinians), and ~ 0.2 more Arthropods (units: individuals m^{-2}).

3.4. Induction time

The *Porites astreoides* selected for analysis were surrounded by octocoral canopies with mean heights of 33.3 ± 1.8 cm, 29.6 ± 2.7 cm, and 37.5 ± 5.0 cm (all ± SEM, n = 6–8 quadrats) at Cabritte Horn, Tektite, and White Point, respectively. The mean densities of octocorals forming these canopies were 10.3 ± 1.3 individuals m^{-2} at Cabritte Horn, 4.6 ± 0.6 individuals m^{-2} at Tektite, and 7.4 ± 1.4 individuals m^{-2} at White Point (all ± SEM, n = 6–8 quadrats), with mean canopy closure values of 51.2 ± 8.7%, 50.0 ± 8.5%, and 44.0 ± 9.1% (all ± SEM, n = 6–8 quadrats), respectively. Twelve *P. astreoides* were sampled for induction time at Cabritte Horn, 16 at Tektite, and 14 at White Point.

All induction curves had similar shapes (Fig. S1). Following the initial measurements of fluorescence, basal fluorescence (F_o) ranged from 190 to 711 and maximal fluorescence (F_m) from 412 to 1767; following the longest exposure to actinic light (i.e., 17 min), $F_{o'}$ ranged from 109 to 343 and $F_{m'}$ from 164 to 467. rETR calculated from these values varied as a logarithmic function of exposure to actinic light that usually (35 of 42 cases) reached a plateau in 17 min. rETR rapidly increased with duration of exposure to actinic light up to 4.25 min, but with longer exposures, increased more slowly. For 41 of 42 colonies, the highest rate of increase in rETR occurred during the first three minutes of exposure to actinic light. For seven of the corals, rETR did not reach a plateau as a function of exposure to light and continued to increase with time; in two cases, rETR declined with time after reaching a maximum value. The mean asymptotic rETR did not significantly differ across sites ($F_{2,36} = 1.041$, $P = 0.363$), canopy treatment ($F_{1,2} = 1.219$, $P = 0.385$), or their interaction ($F_{2,36} = 0.242$, $P = 0.242$) (Fig. 7).

Based on the intersection of the initial slope of the curve and the mean rETR of the last three time points, induction time (i.e., T_i) varied from 1.2 to 5.0 min for understory corals, and from 2.4 to 6.5 min for open reef corals. T_i was unaffected by the interaction between site and canopy ($F_{2,36} = 0.064$, $P = 0.939$), or the main effects of site ($F_{2,36}$ =

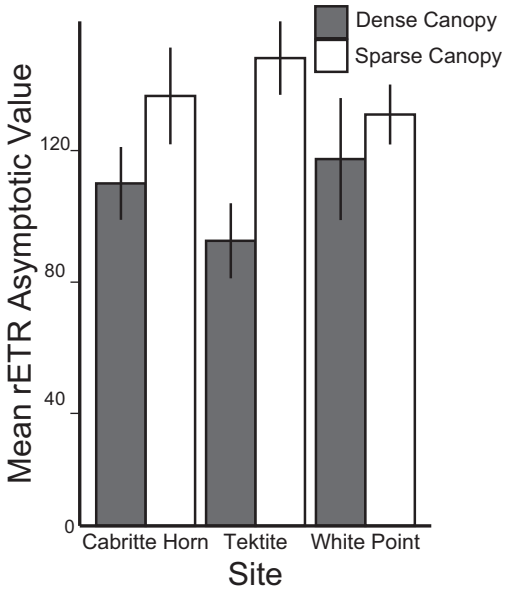

Fig. 7. Bar graph of the mean (± SE) asymptotic rETR value of *Porites astreoides* in dense and sparse octocoral canopies at 7.0–7.9-m depth, at Cabritte Horn (n = 6 per canopy type), Tektite (n = 8 per canopy type), and White Point (n = 7 per canopy type).

0.506, $P = 0.607$), and canopy ($F_{1,2} = 1.778$, $P = 0.314$). Pooling of results for *P. astreoides* among sites and canopy location (under dense canopies versus outside of dense canopies) showed that the mean induction time was 3.5 ± 0.1 min (± SEM, $n = 42$, Fig. 6).

4. Discussion

4.1. Overview

We found that the benthic invertebrate community in the understory habitat of octocoral forests was associated with canopy formation. The understory habitat was physically distinguished from the habitat adjacent to areas of sparse colonies through the presence of sunflecks. However, the induction time of the reef coral *Porites astreoides* suggests photosynthetic organisms in the understory habitat were not physiologically adjusted to utilize a dynamic light regime compared to organisms in habitats with sparse octocoral colonies. Together, these results suggest that arborescent octocorals creating dense canopies function as autogenic ecosystem engineers (sensu Jones et al., 1994) by modifying features of the physical environment (here, the dynamic light regime) affecting the understory habitat. One outcome of these effects is to drive changes in the benthic invertebrate community in the understory habitat, relative to the more open reef habitat. The effect on dynamic light availability augments the well-known mechanisms by which underwater biogenic canopies modify seawater flow (Ghisalberti and Nepf, 2006; Nepf, 2012b) and the quantity of light (i.e., shading) (Gerard, 1984; Stewart et al., 2007).

4.2. Community beneath canopies

Interpretation of the present effects of the octocoral canopy on the understory invertebrate community requires consideration of the influence of the two major hurricanes that impacted these reefs in 2017, 22 months before this study began (e.g., described in Edmunds, 2019). Although the percentage cover of stony corals was not greatly affected by these storms (Edmunds, 2019), the abundance of other taxa including sponges and octocorals was depressed (Edmunds et al., 2020; Lasker et al., 2020a), and it is reasonable to expect that a diverse array of delicate, erect, and mobile taxa were removed from shallow reefs by storm waves. We do not know the magnitude of this effect on the overall assemblages of benthic invertebrates on the shallow reefs of St. John, or the extent to which they may have recovered in the 22 months following the storms. Therefore, we cannot exclude the possibility that the effects of octocoral canopies on the understory invertebrate communities described herein are unique to the years in which the surveys were conducted. However, the broad spectrum of effects of octocoral forests on benthic invertebrates beneath their canopies (e.g., Fig. 5, Table S2.), which included scleractinians, suggests that the direction of the effect is not an artifact of the disturbance regime prior to this study (i.e., the hurricanes in 2017). We recognize that the same may not be true for the magnitude of this effect, which may have been attenuated by the effects of the storms in removing invertebrates from the study reefs.

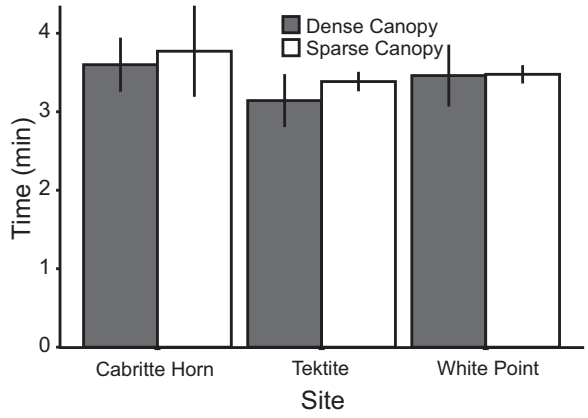

Fig. 6. Bar graph of the mean induction time (± SE) of *Porites astreoides* in dense and sparse octocoral canopies at 7.0–7.9 m depth, at Cabritte Horn ($n = 6$ per canopy type), Tektite ($n = 8$ per canopy type), and White Point ($n = 7$ canopy type).

When the present study reefs were surveyed in 2019 and 2020, they provided examples of octocoral forests that had been thinned by disturbance, yet retained their emergent properties and the population structure of its autogenic engineer (i.e., octocorals). On these reefs, immediately following Hurricanes Irma and Maria in 2017, the densities of octocorals were reduced by 23–47% while the relative abundance of octocoral species was preserved (Edmunds, 2020; Lasker et al., 2020a). By 2019, octocorals were recruiting on these reefs at densities similar to those recorded prior to the storms (Lasker et al., 2020a). Therefore, the ecological significance of the hurricane-related declines in population sizes of octocorals was reduced through preservation of relative abundances by species, and through the quick replacement of octocoral colonies by recruitment. Further, based on published growth rates of multiple octocoral genera (Kupfner Johnson and Hallock, 2020) the canopy heights recorded in the present study would be established by colonies ~11 years old (i.e., they recruited years before Hurricanes Irma and Maria). Therefore, it is likely that the canopies, although thinned by these hurricanes, retained their pre-disturbance emergent properties including the ability to influence the benthic communities in their understory habitat.

The multivariate features of octocoral canopies and the multivariate invertebrate community structure in the understory habitats were correlated at Cabritte Horn and White Point. These results suggest that octocoral forests in St. John are affecting invertebrate community composition beneath their canopies, while themselves contributing to a broader cryptic regime change affecting the shallow reefs of St. John (Edmunds and Lasker, 2016). Prior to this study, octocoral abundances were increasing on the study reefs (Lenz et al., 2015), and there was evidence of a cryptic regime change (sensu Hughes et al., 2013)) in the benthic community composed of scleractinians and octocorals (Edmunds and Lasker, 2016). The present study augments the findings of Edmunds and Lasker (2016), by showing that octocoral forests modify the taxonomic composition and abundance of invertebrates in the understory benthic community. Based on the changes we detected (Table S2), it is likely that these effects would not be readily detected through casual inspection (e.g., while swimming over the reef), yet the subtle changes could amount to ecologically significant effects. Evaluating the functional significance of the effects of octocoral forests on the biota with which they associate (and modify) is likely to be a productive topic for future research.

Our results emerged through an analysis of canopies studied across a gradient of octocoral densities. A limitation of testing our key hypotheses regarding the effects of octocoral canopies is that arborescent octocorals are so common on these shallow reefs (Lasker et al., 2020a, 2020b), that areas without arborescent octocorals (i.e., "open reef") are effectively absent. This constituted an experimental limitation for our study (i.e., there was not an octocoral-free area of reef with which dense octocoral forests could be contrasted) that was addressed by exploiting the natural gradient of octocoral densities to support a contrast of dense (> 5 octocorals m^{-2}) and sparse (≤ 5 octocorals m^{-2}) colonies. The rationale for this distinction was provided by evidence that "canopy effects" emerged at >5–7 octocorals m^{-2} (present study; Lasker et al., 2020b; Tsounis et al., 2020; Cerpovicz and Lasker, 2021). To evaluate the implications of this categorization on our conclusions, the contrast of canopy effects was repeated using a more conservative distinction between dense (i.e., > 7 octocorals m^{-2}) and sparse (i.e., < 3 octocorals m^{-2}) canopies. With this distinction, an effect of dense canopies on the benthic invertebrate communities was still detected (Cabritte Horn: $P = 0.026$, Mantel $r = 0.223$), suggesting that the effect detected with a more

liberal definition of dense octocoral canopies was biologically meaningful.

The absence of a relationship between octocoral forests and the invertebrate community structure within the understory habitat at Tektite suggests that the relationship between the two is influenced by local environmental conditions. Relative to White Point and Cabritte Horn, Tektite is sheltered from the prevailing regimes of wind and waves (CariCOOS buoy 41,052). Calmer conditions at Tektite likely attenuated the differences in physical environmental conditions (e.g., wave forces and flow speed) in understory habitats versus areas of sparse octocoral colonies, thus favoring similar benthic invertebrate communities between these two habitats.

Overall, the effect of water motion on octocorals provides a parsimonious explanation for the present results. Ambient flow speeds are likely to interact with the structure of octocoral forests to modulate the consequences of canopy formation on the community structure of benthic invertebrates. Water motion mediates the swaying of arborescent octocoral colonies (and sunflecking [this study]), turbulence within the canopy (Lasker et al., 2020b), sedimentation (Tsounis et al., 2018; Cerpovicz and Lasker, 2021), octocoral recruitment (Privitera-Johnson et al., 2015), and for suspension feeders, food abundance (Abelson et al., 1993) and particle capture (Okamura, 1984, 1985; Helmuth and Sebens, 1993; Sebens et al.,1997). Therefore, under conditions that reduce interactions between octocorals and seawater flow, for example, where octocorals occur at sparse densities and do not form a distinct canopy, or where seawater motion is locally attenuated (e.g., at Tektite), an effect of octocoral forests on understory invertebrates is likely to be weakened.

4.3. Light regime beneath canopies and induction time

In the present study, octocoral forests altered understory light by increasing the occurrence of sunflecks lasting ~5–30 s relative to areas with sparse octocoral colonies. Therefore, a priori, it was reasonable to expect that photoautotrophs within this habitat might display changes in their photophysiology to exploit this source of energy (as occurs in terrestrial forests [Zipperlen and Press, 1997]). Despite this expectation, the induction time of a common coral was not different with respect to the presence of dense or sparse octocoral colonies. Given the reduction in light energy (PFD) that occurs within octocoral forests (i.e., through shading), it is possible that shade adaptation (sensu Boardman, 1977), as opposed to a capacity for dynamic photosynthesis, may be more important in structuring these photoautotrophic understory communities. In St. John, dense octocoral forests reduced light by 36% on the luminance scale (i.e., lux), and by 34% on the PAR scale (i.e., μmol photons m^{-2} s^{-1}), which is of a magnitude sufficient to induce shade adaptation in corals (Anthony et al., 2005; Todd, 2008).

4.4. Conclusions

This research, as well as recent studies (Lasker et al., 2020b; Cerpovicz and Lasker, 2021), indicates that arborescent octocorals can function as autogenic ecosystem engineers (sensu Jones et al., 1994) by forming dense animal forests. In this way (see also Kupfner Johnson and Hallock, 2020; Lasker et al., 2020b; Cerpovicz and Lasker, 2021), dense octocoral forests have similarities to many other types of forests (e.g., trees, kelp, and seagrass). Despite growing awareness of the importance of octocoral forests (Lasker et al., 2020b), there remains little quantitative information on the "canopy effect" created by dense stands of arborescent octocorals, particularly with regards to the effects of the physical and biological features of the understory habitat. The present study suggests that further exploration of these effects is likely to be valuable in describing the holistic implications of the ongoing changes in the benthic taxa dominating Caribbean coral reefs.

Supplementary data to this article can be found online at https://doi.org/10.1016/j.jembe.2023.151870.

CRediT authorship contribution statement

John F. Girard: Conceptualization, Methodology, Validation, Formal analysis, Investigation, Resources, Data curation, Writing – original draft, Writing – review & editing, Visualization, Supervision, Funding acquisition. **Peter J. Edmunds:** Conceptualization, Methodology, Validation, Resources, Writing – original draft, Writing – review & editing, Supervision, Project administration, Funding acquisition.

Declaration of Competing Interest

The authors declare that they have no known competing financial interests or personal relationships that could have appeared to influence the work reported in this paper.

Data availability

Data available at bc0dmo (https://www.bco-dmo.org/) project 825192 data DOIs xxx, xxx, xxx, xxx, xxx, xxx, xxx, xxx, xxx, and xxx.

Acknowledgements

This research was funded by grants from the United States National Science Foundation (OCE 20-19992, OCE 17-56678, DEB 13-50146) as well as the CSUN Graduate Studies Thesis Support Program. Work within the Virgin Islands National Park was approved under permits (VIIS-2019-SCI-0022, VIIS-2021-SCI-0001). We thank M. Williams, L. Stockton, E. Lenz, C. Didden, N. Bean, and K. Wong for their support in the field. H.R. Lasker, L. Bramanti, and G. Tsounis provided input regarding dynamics of octocoral communities, and R.C. Carpenter, K. Nickols, C. terHorst, and four anonymous reviewers provided comments that improved earlier drafts of this manuscript. Sections of this manuscript were submitted to CSUN for partial fulfillment of J.F. Girard's Masters Thesis. This is contribution number 374 of the CSUN marine biology program.

References

Abelson, A., Miloh, T., Loya, Y., 1993. Flow patterns induced by substrata and body morphologies of benthic organisms, and their roles in determining availability of food particles. Limnol. Oceanogr. 38, 1116–1124. https://doi.org/10.4319/lo.1993.38.6.1116.

Ackerman, J.D., Okubot, A., 1993. Reduced mixing in a marine macrophyte canopy. Funct. Ecol. 7, 305–309. https://doi.org/10.2307/2390209.

Anthony, K.R.N., Hoogenboom, M.O., Connolly, S.R., 2005. Adaptive variation in coral geometry and the optimization of internal colony light climates. Funct. Ecol. 19, 17–26. https://doi.org/10.1111/j.0269-8463.2005.00925.x.

Atkinson, M.J., Falter, J.L., 2003. Coral Reefs. In: Black, K., Graham, S. (Eds.), Biogeochemistry of Marine Systems. CRC Press, Boca Raton, pp. 40–64.

Boardman, N.K., 1977. Comparative photosynthesis of sun and shade plants. Annu. Rev. Plant Physiol. 28, 355–377. https://doi.org/10.1146/annurev.pp.28.060177.002035.

Bradbury, M., Baker, N.R., 1981. Analysis of the slow phases of the in vivo chlorophyll fluorescence induction curve. Biochem. Biophys. Acta 5, 542–551.

Bradbury, M., Baker, N.R., 1984. A quantitative determination of photochemical and non-photochemical quenching during the slow phase of the chlorophyll fluorescence induction curve of bean leaves. BBA-Bioenergetics 765, 275–281. https://doi.org/10.1016/0005-2728(84)90166-X.

Brunel, C., Gros, R., Lerch, T.Z., Da Silva, A.M.F., 2020. Changes in soil organic matter and microbial communities after fine and coarse residues inputs from Mediterranean tree species. Appl. Soil Ecol. 149, 103516 https://doi.org/10.1016/j.apsoil.2020.103516.

Cary, L.R., 1914. Observations upon the growth-rate and oecology of gorgonians. In: Papers from the Tortugas Laboratory of the Carnegie Institution Washington, pp. 79–90.

Cerpovicz, A.F., Lasker, H., 2021. Canopy effects of octocoral communities on sedimentation: modern baffles on the shallow-water reefs of St. Coral Reefs, John, USVI. https://doi.org/10.1130/abs/2018am-320175.

Chazdon, R.L., Fetcher, N., 1984. Light environments of tropical forests. In: Mooney, H. A., Vazquez-Yanes, C. (Eds.), Physiological Ecology of Plants of the Wet Tropics. Oxatepec and Los Tuxtlas, Mexico, pp. 27–36. https://doi.org/10.1007/978-94-009-7299-5_4.

Chazdon, R.L., Pearcy, R.W., 1991. The importance of sunflecks for forest understory plants. Bioscience 41, 760–766. https://doi.org/10.2307/1311725.

Clarke, K.R., Ainsworth, M., 1993. A method of linking multivariate community structure to environmental variables. Mar. Ecol. Prog. Ser. 92, 205–219. https://doi.org/10.3354/meps092205.
Clarke, K.R., Somerfield, P.J., Gorley, R.N., 2008. Testing of null hypotheses in exploratory community analyses: similarity profiles and biota-environment linkage. J. Exp. Mar. Biol. Ecol. 366, 56–69. https://doi.org/10.1016/j.jembe.2008.07.009.
Clendenning, K.A., Haxo, F.T., 1956. Photosynthetic induction in marine algae. Can. J. Bot. 34, 214–230.
Collier, C.J., Waycott, M., Ospina, A.G., 2012. Responses of four Indo-West Pacific seagrass species to shading. Mar. Pollut. Bull. 65, 342–354. https://doi.org/10.1016/j.marpolbul.2011.06.017.
Denny, M.W., Daniel, T.L., Koehl, M.A.R., 1985. Mechanical limits to size in wave-swept organisms. Ecol. Monogr. 55, 69–102.
Edmunds, P.J., 2019. Three decades of degradation lead to diminished impacts of severe hurricanes on Caribbean reefs. Ecology 100, 1–10. https://doi.org/10.1002/ecy.2587.
Edmunds, P.J., 2020. High ecological resilience of the sea fan *Gorgonia ventalina* during two severe hurricanes. PeerJ 8. https://doi.org/10.7717/peerj.10315.
Edmunds, P.J., Lasker, H.R., 2016. Cryptic regime shift in benthic community structure on shallow reefs in St. John, US Virgin Islands. Mar. Ecol. Prog. Ser. 559, 1–12. https://doi.org/10.3354/meps11900.
Edmunds, P.J., Tsounis, G., Lasker, H.R., 2016. Differential distribution of octocorals and scleractinians around St. John and St. Thomas, US Virgin Islands. Hydrobiologia 767, 347–360. https://doi.org/10.1007/s10750-015-2555-z.
Edmunds, P.J., Tsounis, G., Boulon, R., Bramanti, L., 2018. Long-term variation in light intensity on a coral reef. Coral Reefs 37, 955–965. https://doi.org/10.1007/s00338-018-1721-y.
Edmunds, P.J., Coblentz, M., Wulff, J., 2020. A quarter-century of variation in sponge abundance and community structure on shallow reefs in St. John, US Virgin Islands. Mar. Biol. 167, 1–17. https://doi.org/10.1007/s00227-020-03740-8.
Emery, W.J., Thomson, R.E., 2014. Time-series analysis methods. In: Emery, W.J., Thomson, R.E. (Eds.), Data Analysis Methods in Physical Oceanography. Elsevier, pp. 404–494.
Fox, R.J., Bellwood, D.R., 2013. Niche partitioning of feeding microhabitats produces a unique function for herbivorous rabbitfishes (Perciformes, Siganidae) on coral reefs. Coral Reefs 32, 13–23. https://doi.org/10.1007/s00338-012-0945-5.
Fox, J., Weisberg, S., 2019. An {R} Companion to Applied Regression, Third edition. Sage, Thousand Oaks CA. URL: https://socialsciences.mcmaster.ca/jfox/Books/Companion/.
Fung, T., Seymour, R.M., Johnson, C.R., 2011. Alternative stable states and phase shifts in coral reefs under anthropogenic stress. Ecology 92, 967–982. https://doi.org/10.1890/10-0378.1.
Genty, B., Briantais, J.M., Baker, N.R., 1989. The relationship between the quantum yield of photosynthetic electron transport and quenching of chlorophyll fluorescence. Biochem. Biophys. Acta - Gen. Subj. 990, 87–92. https://doi.org/10.1016/S0304-4165(89)80016-9.
Gerard, V.A., 1984. The light environment in a giant kelp forest: influence of *Macrocystis pyrifera* on spatial and temporal variability. Mar. Biol. 84, 189–195. https://doi.org/10.1007/BF00393004.
Ghisalberti, M., Nepf, H., 2006. The structure of the shear layer in flows over rigid and flexible canopies. Environ. Fluid Mech. 6, 277–301. https://doi.org/10.1007/s10652-006-0002-4.
Giuliani, R., Brown, K.J., 2008. Within-canopy sampling of global irradiance to describe downwelling light distribution and infer canopy stratification in a broadleaf forest. Tree Physiol. 28, 1407–1419. https://doi.org/10.1093/treephys/28.9.1407.
GoPro, 2013. Hero 3 silver edition: user manual. 1–62. https://gopro.com/content/dam/help/hero3-silver-edition/manuals/HERO3_Silver_UM_ENG_RevC_web.pdf. Accessed: 21/Dec/2022.
Guy-Haim, T., Lyons, D.A., Kotta, J., Ojaveer, H., Queirós, A.M., Chatzinikolaou, E., Arvanitidis, C., Como, S., Magni, P., Blight, A.J., Orav-Kotta, H., Somerfield, P.J., Crowe, T.P., Rilov, G., 2018. Diverse effects of invasive ecosystem engineers on marine biodiversity and ecosystem functions: a global review and meta-analysis. Glob. Chang. Biol. 24, 906–924. https://doi.org/10.1111/gcb.14007.
Heinz Walz, G., 1998. UNDERWATER FLUOROMETER submersible photosynthesis yield analyzer handbook of operation, 1st ed. Effeltrich.
Helmuth, B., Sebens, K., 1993. The influence of colony morphology and orientation to flow on particle capture by the scleractinian coral *Agaricia agaricites* (Linnaeus). J. Exp. Mar. Biol. Ecol. 165, 251–278. https://doi.org/10.1016/0022-0981(93)90109-2.
Hilmers, T., Friess, N., Bässler, C., Heurich, M., Brandl, R., Pretzsch, H., Seidl, R., Müller, J., 2018. Biodiversity along temperate forest succession. J. Appl. Ecol. 55, 2756–2766. https://doi.org/10.1111/1365-2664.13238.
Hughes, T.P., Linares, C., Dakos, V., van de Leemput, I.A., van Nes, E.H., 2013. Living dangerously on borrowed time during slow, unrecognized regime shifts. Trends Ecol. Evol. 28, 149–155. https://doi.org/10.1016/j.tree.2012.08.022.
Humann, P., Deloach, N., Wilk, L., 2013. Reef Creature Identification: Florida Caribbean Bahamas, 3rd ed. New World Publications.
Jennings, S.B., Brown, N.D., Sheil, D., 1999. Assessing forest canopies and understory illumination: canopy closure, canopy cover and other measures. Forestry 72, 59–73. https://doi.org/10.1093/forestry/72.1.59.
Jones, C.G., Lawton, J.H., Shachak, M., 1994. Organisms as ecosystem engineers. Oikos 69, 373. https://doi.org/10.2307/3545850.
Kaiser, E., Morales, A., Harbinson, J., Kromdijk, J., Heuvelink, E., Marcelis, L.F.M., 2015. Dynamic photosynthesis in different environmental conditions. J. Exp. Bot. 66, 2415–2426. https://doi.org/10.1093/jxb/eru406.
Kaiser, E., Kromdijk, J., Harbinson, J., Heuvelink, E., Marcelis, L.F.M., 2017. Photosynthetic induction and its diffusional, carboxylation and electron transport processes as affected by CO2 partial pressure, temperature, air humidity and blue irradiance. Ann. Bot. 119, 191–205. https://doi.org/10.1093/aob/mcw226.
Kern, C.C., Montgomery, R.A., Reich, P.B., Strong, T.F., 2013. Canopy gap size influences niche partitioning of the ground-layer plant community in a northern temperate forest. J. Plant Ecol. 6, 101–112. https://doi.org/10.1093/jpe/rts016.
Kinzie, R.A., 1973. The zonation of West Indian gorgonians. Bull. Mar. Sci. 23, 93–155.
Kirk, J.T.O., 1977. Attenuation of light in natural waters. Mar. Freshw. Res. 28, 497–508. https://doi.org/10.1071/MF9770497.
Koehl, M.A.R., 1982. The interaction of moving water and sessile organisms. Sci. Am. https://doi.org/10.1038/scientificamerican1282-124.
Kramer, P.A., Kramer, P.R., Ginsburg, R.N., 2003. Assessment of the Andros Island reef system, Bahamas (Part 1: stony corals and algae). Atoll Res. Bull. 78–99.
Kupfner Johnson, S., Hallock, P., 2020. A review of symbiotic gorgonian research in the Western Atlantic and Caribbean with recommendations for future work. Coral Reefs 39, 239–258. https://doi.org/10.1007/s00338-020-01891-0.
Lasker, H.R., Martínez-Quintana, Bramanti, L., Edmunds, P.J., 2020a. Resilience of octocoral forests to catastrophic storms. Sci. Rep. 10, 1–8. https://doi.org/10.1038/s41598-020-61238-1.
Lasker, Howard R., Bramanti, L., Tsounis, G., Edmunds, P.J., 2020b. The rise of octocoral forests on Caribbean reefs. In: Advances in Marine Biology. Elsevier Ltd. https://doi.org/10.1016/bs.amb.2020.08.009
Lenz, E.A., Bramanti, L., Lasker, H.R., Edmunds, P.J., 2015. Long-term variation of octocoral populations in St. John, US Virgin Islands. Coral Reefs 34, 1099–1109. https://doi.org/10.1007/s00338-015-1315-x.
Lin, M.C., Dai, C.F., 1996. Drag, morphology and mechanical properties of three species of octocorals. J. Exp. Mar. Biol. Ecol. 201, 13–22. https://doi.org/10.1016/0022-0981(95)00199-9.
Long, M.H., Rheuban, J.E., Berg, P., Zieman, J.C., 2012. A comparison and correction of light intensity loggers to photosynthetically active radiation sensors. Limnol. Oceanogr. Methods 10, 416–424. https://doi.org/10.4319/lom.2012.10.416.
Lowe, R.J., Falter, J.L., 2015. Oceanic forcing of coral reefs. Annu. Rev. Mar. Sci. 7, 43–66. https://doi.org/10.1146/annurev-marine-010814-015834.
Luhar, M., Nepf, H.M., 2011. Flow-induced reconfiguration of buoyant and flexible aquatic vegetation. Limnol. Oceanogr. 56, 2003–2017. https://doi.org/10.4319/lo.2011.56.6.2003.
Macintyre, H.L., Kana, T.M., Geider, R.J., 2000. The effect of water motion on short-term rates of photosynthesis by marine phytoplankton. Trends Plant Sci. 5, 12–17. https://doi.org/10.1016/S1360-1385(99)01504-6.
Madin, J.S., Baird, A.H., Dornelas, M., Connolly, S.R., 2014. Mechanical vulnerability explains size-dependent mortality of reef corals. Ecol. Lett. 17, 1008–1015. https://doi.org/10.1111/ele.12306.
Miller, R.J., Lafferty, K.D., Lamy, T., Kui, L., Rassweiler, A., Reed, D.C., 2018. Giant kelp, *Macrocystis pyrifera*, increases faunal diversity through physical engineering. Proc. R. Soc. B Biol. Sci. 285 https://doi.org/10.1098/rspb.2017.2571.
Monismith, S.G., 2007. Hydrodynamics of coral reefs. Annu. Rev. Fluid Mech. 39, 37–55. https://doi.org/10.1146/annurev.fluid.38.050304.092125.
Müllner, D., 2013. fastcluster: Fast hierarchical, agglomerative clustering routines for R and Python. J. Stat. Softw. 53, 1–18.
Mumby, P.J., 2009. Phase shifts and the stability of macroalgal communities on Caribbean coral reefs. Coral Reefs 28, 761–773. https://doi.org/10.1007/s00338-009-0506-8.
Nepf, H.M., 2012a. Hydrodynamics of vegetated channels. J. Hydraul. Res. 50, 262–279. https://doi.org/10.1080/00221686.2012.696559.
Nepf, H.M., 2012b. Flow and transport in regions with aquatic vegetation. Annu. Rev. Fluid Mech. 44, 123–142. https://doi.org/10.1146/annurev-fluid-120710-101048.
Nishizaki, M.T., Carrington, E., 2014. The effect of water temperature and flow on respiration in barnacles: patterns of mass transfer versus kinetic limitation. J. Exp. Biol. 217, 2101–2109. https://doi.org/10.1242/jeb.101030.
Nobel, P., 2020. Physicochemical and Environmental Plant Physiology, 5th ed. Academic Press, San Diego.
Okamura, B., 1984. The effects of ambient flow velocity, colony size, and upstream colonies on the feeding success of bryozoa. I. *Bugula stolonifera* Ryland, an arborescent species. J. Exp. Mar. Biol. Ecol. 83, 179–193. https://doi.org/10.1016/0022-0981(84)90044-3.
Okamura, B., 1985. The effects of ambient flow velocity, colony size, and upstream colonies on the feeding success of bryozoa. II. *Conopeum reticulum* (Linnaeus), an encrusting species. J. Exp. Mar. Biol. Ecol. 89, 69–80. https://doi.org/10.1016/0022-0981(85)90082-6.
Oksanen, J., Guillaume, B.F., Friendly, M., Kindt, R., Legendre, P., McGlinn, D., Minchin, P.R., O'Hara, R.B., Simpson, G.L., Solymos, P., Stevens, M.H.H., Szoecs, E., Wagner, H., 2019. vegan: Community Ecology Package. R package version 2.5-6. https://CRAN.R-project.org/package=vegan.
Osterhout, W.J.V., Haas, A.R.C., 1918. Dynamical aspects of photosynthesis. Proc. Natl. Acad. Sci. 4, 85–91. https://doi.org/10.1073/pnas.4.4.85.
Pahl-wostl, C., Imboden, D.M., 1990. DYPHORA-a dynamic model for the rate of photosynthesis of algae. J. Plankton Res. 12, 1207–1221. https://doi.org/10.1093/plankt/12.6.1207.
Pearcy, R.W., 1988. Photosynthetic utilization of lightflecks by understory plants. Aust. J. Plant Physiol. 15, 223–238. https://doi.org/10.1071/pp9880223.
Pearcy, R.W., Osteryoung, K., Calkin, H.W., 1985. Photosynthetic responses to dynamic light environments by Hawaiian trees. Plant Physiol. 79, 896–902. https://doi.org/10.1104/pp.79.3.896.

Poorter, L., Oberbauer, S.F., 1993. Photosynthetic induction responses of two rainforest tree species in relation to light environment. Oecologia 96, 193–199. https://doi.org/10.1007/BF00317732.

Privitera-Johnson, K., Lenz, E.A., Edmunds, P.J., 2015. Density-associated recruitment in octocoral communities in St. John, US Virgin Islands. J. Exp. Mar. Biol. Ecol. 473, 103–109. https://doi.org/10.1016/j.jembe.2015.08.006.

Rossi, S., Bramanti, L., Gori, A., Orejas, C., 2017. Marine Animal Forests: The Ecology of Benthic Biodiversity Hotspots, Marine Animal Forests. Springer Nature, Cham, Switzerland. https://doi.org/10.1007/978-3-319-17001-5_17-2.

Ruzicka, R.R., Colella, M.A., Porter, J.W., Morrison, J.M., Kidney, J.A., Brinkhuis, V., Lunz, K.S., MacAulay, K.A., Bartlett, L.A., Meyers, M.K., Colee, J., 2013. Temporal changes in benthic assemblages on Florida Keys reefs 11 years after the 1997/1998 El Niño. Mar. Ecol. Prog. Ser. 489, 125–141. https://doi.org/10.3354/meps10427.

Schneider, C.A., Rasband, W.S., Eliceiri, K.W., 2012. NIH Image to ImageJ: 25 years of image analysis. Nat. Methods 9. https://doi.org/10.1038/nmeth.2089, 676–675.

Schreiber, U., Gademann, R., Ralph, P.J., Larkum, A.W.D., 1997. Assessment of photosynthetic performance of Prochloron in *Lissoclinum patella* in hospite by chlorophyll fluorescence measurements. Plant Cell Physiol. 38, 945–951. https://doi.org/10.1093/oxfordjournals.pcp.a029256.

Sebens, K.P., Witting, J., Helmuth, B., 1997. Effects of water flow and branch spacing on particle capture by the reef coral *Madracis mirabills* (Duchassaing and Michelotti). J. Exp. Mar. Biol. Ecol. 211, 1–28. https://doi.org/10.1016/S0022-0981(96)02636-6.

Seilmayer, M., 2019. spectral: Common Methods of Spectral Data Analysis. Package version 1.3. https://CRAN.R-project.org/package=spectral.

Shelamoff, V., Layton, C., Tatsumi, M., Cameron, M.J., Wright, J.T., Johnson, C.R., 2019. Patch size and density of canopy-forming kelp modify influences of ecosystem engineering on understory algal and sessile invertebrate assemblages. Mar. Ecol. Prog. Ser. 632, 59–79. https://doi.org/10.3354/meps13155.

Siebert, T., Branch, G.M., 2006. Ecosystem engineers: interactions between eelgrass *Zostera capensis* and the sandprawn *Callianassa kraussi* and their indirect effects on the mudprawn *Upogebia africana*. J. Exp. Mar. Biol. Ecol. 338, 253–270. https://doi.org/10.1016/j.jembe.2006.06.024.

Somerfield, P.J., Clarke, K.R., 2013. Inverse analysis in non-parametric multivariate analyses: distinguishing groups of associated species which covary coherently across samples. J. Exp. Mar. Biol. Ecol. 449, 261–273. https://doi.org/10.1016/j.jembe.2013.10.002.

Stewart, H.L., Payri, C.E., Koehl, M.A.R., 2007. The role of buoyancy in mitigating reduced light in macroalgal aggregations. J. Exp. Mar. Biol. Ecol. 343, 11–20. https://doi.org/10.1016/j.jembe.2006.10.031.

Stramska, M., Dickey, T.D., 1998. Short-term variability of the underwater light field in the oligotrophic ocean in response to surface waves and clouds. Deep. Res. Part I Oceanogr. Res. Pap. 45, 1393–1410. https://doi.org/10.1016/S0967-0637(98)00020-X.

Suggett, D.J., Moore, C.M., Geider, R.J., 2010. Estimating aquatic productivity from active fluorescence measurements. In: Suggett, D.J., Borowitzka, M.A., Prasil, O. (Eds.), Chlorophyll a Fluorescence in Aquatic Sciences: Methods and Applications. Springer, Netherlands, pp. 104–127. https://doi.org/10.1007/978-90-481-9268-7.

Thorson, G., 1964. Light as an ecological factor in the dispersal and settlement of larvae of marine bottom invertebrates. Ophelia 1, 167–208. https://doi.org/10.1080/00785326.1964.10416277.

Todd, P.A., 2008. Morphological plasticity in scleractinian corals. Biol. Rev. 83, 315–337. https://doi.org/10.1111/j.1469-185X.2008.00045.x.

Tomasko, D.A., 1992. Variation in growth form of shoal grass (*Halodule wrightii*) due to changes in the spectral composition of light below a canopy of turtle grass (*Thalassia testudinum*). Estuaries 15, 214–217. https://doi.org/10.2307/1352694.

Tsounis, G., Edmunds, P.J., 2017. Three decades of coral reef community dynamics in St. John, USVI: a contrast of scleractinians and octocorals. Ecosphere 8. https://doi.org/10.1002/ecs2.1646.

Tsounis, G., Edmunds, P.J., Bramanti, L., Gambrel, B., Lasker, H.R., 2018. Variability of size structure and species composition in Caribbean octocoral communities under contrasting environmental conditions. Mar. Biol. 165, 1–14. https://doi.org/10.1007/s00227-018-3286-2.

Tsounis, G., Steele, M.A., Edmunds, P.J., 2020. Elevated feeding rates of fishes within octocoral canopies on Caribbean reefs. Coral Reefs 39, 1299–1311. https://doi.org/10.1007/s00338-020-01963-1.

Whitaker, D., Christman, M., 2014. clustsig: Significant cluster analysis. R package version 1.1. https://CRAN.R-project.org/package=clustsig.

Wing, S.R., Patterson, M.R., 1993. Effects of wave-induced lightflecks in the intertidal zone of photosynthesis in the macroalgae *Postelsia palmaeformis* and *Hedophyllum sessile* (Phaeophyceae). Mar. Biol. 116, 519–525. https://doi.org/10.1007/BF00350069.

Wing, S.R., Leichter, J.J., Denny, M.W., 1993. A dynamic model for wave-induced light fluctuations in a kelp forest. Limnol. Oceanogr. 38, 396–407. https://doi.org/10.4319/lo.1993.38.2.0396.

Zea, S., Henkel, T.P., Pawlik, J.R., 2014. The Sponge Guide: A Picture Guide to Caribbean Sponges. 3rd edition. https://spongeguide.uncw.edu/index.php (Accessed 21-Dec-2022).

Zipperlen, S.W., Press, M.C., 1997. Photosynthetic Induction and stomatal oscillations in relation to the light environment of two dipterocarp rain forest tree species. J. Ecol. 85, 491–503. https://doi.org/10.2307/2960572.